

Two Anonymous DNA Segments Distinguish the Wilms' Tumor and Aniridia Loci

LISA M. DAVIS, RICHARD STALLARD, GEORGE H. THOMAS, PHILIPPE COUILLIN, CLAUDINE JUNIEN, NORMA J. NOWAK, THOMAS B. SHOWS*

The association of Wilms' tumor with aniridia (the *WAGR* complex) in children with 11p13 chromosomal abnormalities has been established, but the paucity of molecular probes in 11p13 has hampered identification of the responsible genes. Two new anonymous DNA segments have been identified that map to the *WAGR* region of 11p13. Both DNA probes identify a cytologically undetectable deletion associated with a balanced chromosome translocation inherited by a patient with familial aniridia, but not Wilms' tumor. The same two DNA segments are also included in the distal p13-p14.1 deletion of another patient, who has aniridia, Wilms' tumor, and hypogonadism, but they are not included in the p12-p13 deletion of a third patient, who does not have aniridia but has had a Wilms' tumor. The discovery of this aniridia deletion and these two DNA segments that physically separate the Wilms' tumor and aniridia loci should facilitate identification of the genes in the *WAGR* locus, beginning with the aniridia gene.

WILMS' TUMOR IS A NEPHROBLASTOMA that appears in 1:10,000 children (1), and aniridia, complete or partial absence of the iris, appears with a frequency of 1:64,000 to 1:100,000 (2). However, the frequency of aniridia among children with Wilms' tumor increases to 1:50 (3), whereas the frequency of Wilms' tumor among children with aniridia increases to 1:3 (4, 5). The finding that the majority of children with both Wilms' tumor and aniridia have hemizygous constitutional deletions on the short arm of chromosome 11, with 11p13 the region commonly involved, has led to the assignment of the Wilms' tumor-aniridia-genitourinary-mental retardation (*WAGR*) gene complex to 11p13 (5, 6). The genes encoding catalase (*CAT*) and the beta subunit of follicle-stimulating hormone (*FSHB*) have also been assigned to 11p13, at positions flanking the *WAGR* complex (7-10).

Although *CAT* and *FSHB* are the closest known genes to the *WAGR* complex, both have been excluded from the complex because patients have been found who have deletions that leave one of these genes intact (8, 9). To find DNA markers closer to the Wilms' tumor (*WT*) and aniridia (*AN2*) loci, we have isolated and mapped 112 random clones from the chromosome 11 library of the Lawrence Livermore National

Laboratory (11). *WAGR* patients were used to establish a panel of deletion hybrids that separated 11p into nine regions; we were able to assign four of these clones, *D11S89*, *D11S90*, *D11S93*, and *D11S95*, to the subinterval of 11p13, which includes *CAT*, *FSHB*, and the *WAGR* complex. The 11p13 chromosomal abnormalities of three additional patients were characterized with these molecular probes (Fig. 1).

DG-85 is a fibroblast cell line established from the first patient, who has familial aniridia and carries a cytologically balanced translocation between chromosomes 11 and 22 [t(11;22), (p13;q12.2)] (12). RIST is an Epstein-Barr virus (EBV)-transformed lymphoblastoid line established from the second patient, a 9-year-old male who has aniridia and hypogonadism and has had a Wilms' tumor. Our cytological examination of his circulating leukocytes revealed a deletion of distal 11p13-p14.1 (13). DAR 15-14 is a human-mouse somatic cell hybrid established from the third patient, who had Wilms' tumor, but not aniridia, and a deletion of 11p12-p13 (14). This hybrid does not retain the normal chromosome 11.

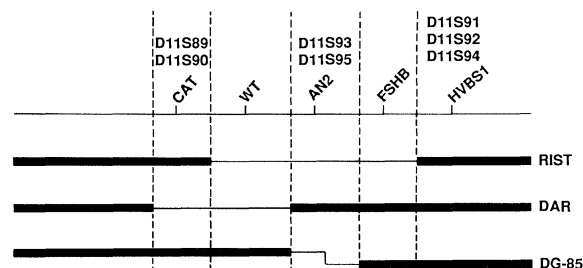
Using somatic cell hybridization, we seg-

regated the DG-85 derivative chromosome 11 and derivative chromosome 22 from each other and from the normal chromosome 11; we also segregated the RIST chromosome 11 with its deletion from its normal homolog (legend to Fig. 2). Somatic cell hybrids segregating these marker chromosomes were examined with *CAT*, *FSHB*, and our DNA markers.

In DG-85, *CAT* (Fig. 2a) and *D11S89* and *D11S90* (13) cosegregated with the derivative 11, and *FSHB* cosegregated with the derivative 22 (Fig. 2a). The other two DNA segments, *D11S93* and *D11S95*, did not cosegregate with either the chromosome 11 derivative or the chromosome 22 derivative (Fig. 2a). Both DNA segments hybridized to DGL4, which retains the normal chromosome 11 (Fig. 2a). Another hybrid retaining both derivative chromosomes together, without the normal chromosome 11, also lacked both *D11S93* and *D11S95* (13). These results suggest that the translocation event was accompanied by a loss of DNA sequences that includes *D11S93* and *D11S95*, that both DNA segments lie between *CAT* and *FSHB*, and that the deleted sequences are entirely contained between *CAT* and *FSHB*.

We also analyzed DG-85, the fibroblast parental cell line, for allele copy number of DNA segments *D11S93* and *D11S95* (Table 1). DNA from DG-85, RIST (a single-dose control, below, and Fig. 2b), and a normal human diploid lymphoblast was hybridized with each of the DNA segment probes, and with a syntenic control, *D11S260* [previously localized to 11q14 (11)]. With the control probe, signals of approximately equal intensity among all three DNA samples were observed, but with *D11S93* and *D11S95*, signals detected in DG-85 were approximately half the intensity of the signal detected in normal human DNA and were approximately equal in intensity to the signal in RIST DNA (Table 1). These results demonstrate that the DNA sequences were not deleted during somatic cell hybridization or growth of the hybrids but, rather, are lacking in the aniridia-translocated deriv-

Fig. 1. The linear order of the anonymous DNA segments, *CAT*, and *FSHB*, and their locations relative to *WT*, *AN2*, and the RIST, DAR 15-14, and DG-85 deletions are summarized. The chromosomes are represented with the centromere to the left. The distal boundary of the DAR 15-14 deletion is drawn identically to the proximal boundary of the DG-85 deletion, because they cannot be distinguished with the available markers. An overlap between the proximal boundaries of RIST and DAR 15-14 is assumed because both patients have had a Wilms' tumor.



L. M. Davis, N. J. Nowak, T. B. Shows, Department of Human Genetics, Roswell Park Memorial Institute, Buffalo, NY 14263.

R. Stallard, Medical Genetics Department, Children's Hospital, Columbus, OH 43205.

G. H. Thomas, Kennedy Institute, and Department of Pediatrics, Johns Hopkins University School of Medicine, Baltimore, MD 21205.

P. Couillin and C. Junien, INSERM, U 73, Château de Longchamp, 75016, Paris, France.

*To whom correspondence should be sent.

Table 1. Densitometric analysis of allele copy number. DNA from normal human lymphoblasts, DG-85 fibroblasts, and R1ST lymphoblasts, digested with Hind III, was hybridized to *D11S93* and *D11S95*. The filters were stripped of the probes and rehybridized with *D11S260*, previously assigned to 11q14 (11).

Cell line	Test probe	Ratio*	Corrected ratio†
R1ST	<i>D11S93</i>	0.52 (0.48, 0.55)	0.45
Normal‡	<i>D11S93</i>	1.15 (1.05, 1.25)	
DG-85	<i>D11S93</i>	0.44 (0.33, 0.54)	0.38
R1ST	<i>D11S95</i>	0.45 (0.42, 0.48)	0.38
Normal‡	<i>D11S95</i>	1.17 (1.16, 1.18)	
DG-85	<i>D11S95</i>	0.54 (0.51, 0.56)	0.46

*Ratios for each test probe were calculated by dividing the signal intensity of the test probe by the signal intensity of the control probe (*D11S260*). The experiments were performed in duplicate, and the analysis of each pair of data was averaged. (The ratios for each member of each pair of duplicates are shown to the right of the averages in parentheses.) †The corrected ratios were calculated by dividing the ratios of the test cell lines by the ratios of the control cell line. ‡The normal control was the human diploid lymphoblast line, GM 0138 (Mutant Cell Repository).

ative chromosomes from DG-85. The results also eliminate the possibility that a complex chromosomal rearrangement has translocated these DNA segments to another chromosomal site. In support of these findings, we have determined that *D11S93* and *D11S95* are present in only one copy each in the cells of the patient's affected son [the proband in (12)] and daughter (13).

A rough estimate of the size of the deletion can be made if one assumes that randomly isolated probes are randomly spaced. Since only two of the 112 chromosome 11 probes we isolated (11) are included in the deleted region, we estimate that the deletion could be as much as 2% (or 3×10^6 bp) of chromosome 11 (thought to be 1.5×10^8 bp). However, we believe that this figure is an overestimate, since the deleted sequences could not be detected cytologically (12). A reasonable lower limit of the deletion size can be estimated: the probability of finding as many as 2 random markers out of 112 from within a deletion less than or equal to 500 kb is less than 0.054.

Previously, somatic cell hybrids derived from an unrelated patient with familial aniridia and a translocation involving 11p13 were analyzed with 11p DNA markers, and no deleted DNA sequences were detected (8). We do not know whether the DNA segments described here are deleted in the patient described earlier, nor do we know the relative positions of the two aniridia-translocation breakpoints. Our findings that *CAT* cosegregates with the chromosome 11 derivative and that *FSHB* cosegregates with the chromosome 22 derivative are consistent with the previous conclusion (8) that *AN2* is

distal to *CAT* and proximal to *FSHB*.

Hybridization analysis also indicated that the chromosome 11 deletion in DAR 15-14 included *CAT* and the aniridia proximal markers *D11S89* and *D11S90*, but did not include *FSHB* or the two DNA segments deleted from the aniridia patient's translocated chromosome 11, *D11S93* and *D11S95* (Fig. 2c). Conversely, the deletion in R1ST included *FSHB* and the same two DNA segments, *D11S93* and *D11S95*, that were deleted from the aniridia patient's translocated chromosome 11. The R1ST deletion did not include *CAT* or the markers proximal to *AN2*, *D11S89*, and *D11S90* (Fig. 2b). The two hybrids that retained the normal chromosome 11 were positive with all six probes (Fig. 2b).

To determine the distal boundary of the R1ST deletion, we also assayed the hybrids with four markers previously assigned (11) to the interval immediately distal to *FSHB*: *HVBS1*, *D11S91*, *D11S92*, and *D11S94*. *HVBS1* is a DNA segment adjacent to a hepatitis B virus integration site (isolated

from a hepatocellular carcinoma), which we previously assigned to 11p13-p14 (15). *HVBS1* and these three markers were all excluded from the R1ST deletion (Fig. 2b, data shown only for *HVBS1* and *D11S92*). Thus, this viral integration site can be excluded from the *WAGR* region of 11p13 and *HVBS1* can be assigned to a position more distal than p14.1, as opposed to its former assignment of p13-p14 (15).

The placement of our anonymous DNA segments, *CAT*, and *FSHB*, relative to the three deletions described here, is summarized in Fig. 1. When these results are considered in light of the phenotypes of the three patients, we are able to conclude the following linear order for the DNA segments and genes in the *WAGR* region of 11p13: CEN-(*CAT*, *D11S89*, *D11S90*)-WT-(*D11S93*, *D11S95*, *AN2*)-(FSHB)-(H*VBS1*, *D11S91*, *D11S92*, *D11S94*)-TEL. These results also firmly establish the gene order CEN-*CAT*-WT-*AN2*-*FSHB*-TEL, as was originally suggested (14).

The DG-85 deletion is a valuable map-

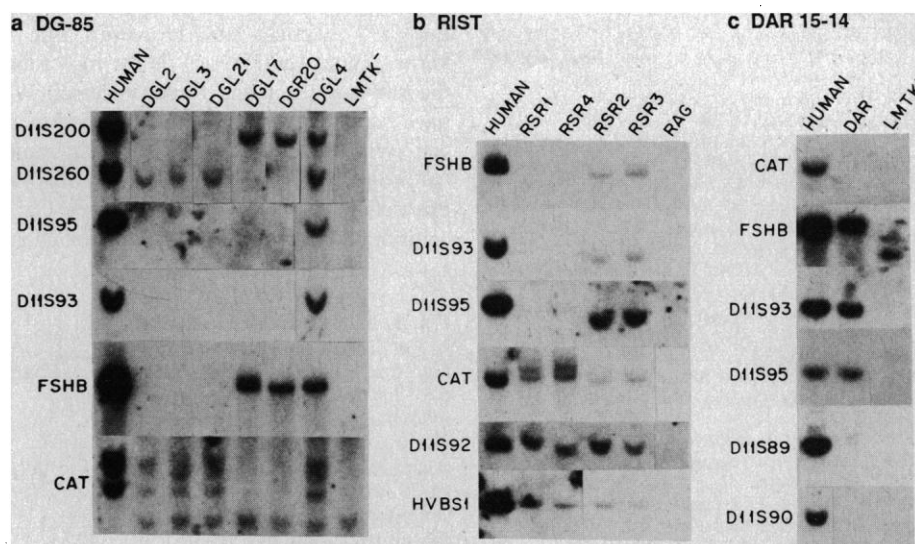


Fig. 2. DNA blot analysis of somatic cell hybrids. Hybridization results for each of the probes (labeled to the left of each panel) are shown. Controls of normal human and mouse (*LM/TK*⁻) are also shown. (a) DG-85 hybrids. DGL2, DGL3, DGL21, DGL17, DGR20, and DGL4 are independent somatic cell isolates. Hybrids carrying the chromosome 11 derivative, the chromosome 22 derivative, or the normal chromosome 11 were identified (top panel) by hybridizing simultaneously with probes *D11S200* and *D11S260*, previously mapped to 11p15 and 11q14, respectively (11). Hybrids DGL2, DGL3, and DGL21 (positive with *D11S260* but not *D11S200*) carry the derivative chromosome 11 (11qter-11p13::22q12.2-22qter). Hybrids DGL17 and DGR20 (positive with *D11S200* but not *D11S260*) carry the derivative chromosome 22 (11pter-11p13::22q12.2-22pter). Hybrid DGL4, positive with both DNA segments, retains the normal chromosome 11. *D11S93* and *D11S95* did not cosegregate with either derivative chromosome. (b) R1ST hybrids. RSR1 and RSR4 are somatic cell hybrids that retain the R1ST chromosome with the 11p deletion, and RSR2 and RSR3 retain the normal chromosome. RAG is the mouse control. The R1ST deletion includes *FSHB*, *D11S93*, and *D11S95*. (c) Hybrid DAR 15-14. The deletion does not include *FSHB*, *D11S93*, or *D11S95*, but does include *CAT*, *D11S89*, and *D11S90*. DG-85 fibroblasts were fused to mouse RAG and *LM/TK*⁻, and R1ST lymphoblasts were fused to mouse RAG cells, as described (16). DNA extractions, Hind III restriction digests, electrophoresis, and transfer to nitrocellulose were as described (17). Probes were radiolabeled by the random primer method (18), and filters were prehybridized, hybridized, washed, and exposed to x-ray film, as described (11). The isolation and characterization of the anonymous DNA segments have been described (11, 19). The *CAT* probe (b and c) was the 800-bp Sca I-Sna BI fragment (20) or (a) pCAT41, a cDNA clone (21). The *FSHB* probe was pFSHB-1.1 (10), and the *HVBS1* probe was S8-2 (15).

ping tool for new DNA markers in the *WAGR* region of 11p13, which will aid in the eventual identification of the Wilms' tumor and aniridia genes. Considering that aniridia and the translocated chromosome have been co-transmitted through at least three generations of this family without any evidence of Wilms' tumor or genitourinary abnormalities, we believe the deletion does not include or disrupt the *WT* gene. This constitutes the first description of a deletion that either disrupts or removes the aniridia gene and clearly spares the Wilms' tumor locus. Therefore markers included in this deletion become likely candidates for the aniridia gene. The DNA segments *D11S93* and *D11S95*, mapping between *CAT* and *FSHB* in a position either very near or within the aniridia gene, should prove to be valuable tools in the eventual identification of the genes involved in the *WAGR* complex, beginning with the aniridia gene.

REFERENCES AND NOTES

1. J. L. Young and R. W. Miller, *J. Pediatr.* **86**, 254 (1975).
2. L. B. Nelson *et al.*, *Surv. Ophthalmol.* **28**, 621 (1984).
3. R. W. Miller *et al.*, *N. Engl. J. Med.* **270**, 922 (1964); K. Narahara *et al.*, *Hum. Genet.* **66**, 181 (1984).
4. J. F. Fraumeni and A. G. Glass, *J. Am. Med. Assoc.* **206**, 825 (1968).
5. H. M. Hittner, V. M. Riccardi, U. Francke, *Ophthalmology* **86**, 1173 (1979).
6. V. M. Riccardi, E. Sujansky, A. C. Smith, U. Francke, *Pediatrics* **61**, 604 (1978); C. Turleau, J. deGrouchy, M.-F. Tournade, M.-F. Gagnadoux, C. Junien, *Clin. Genet.* **26**, 356 (1984); U. Francke, L. B. Holmes, L. Atkins, V. M. Riccardi, *Cytogenet. Cell Genet.* **24**, 185 (1979).
7. C. Junien *et al.*, *Ann. Genet.* **23**, 165 (1980); V. van Heyningen *et al.*, *Proc. Natl. Acad. Sci. U.S.A.* **82**, 8592 (1985).
8. T. Glaser *et al.*, *Nature* **321**, 882 (1986).
9. D. J. Porteous *et al.*, *Proc. Natl. Acad. Sci. U.S.A.* **84**, 5355 (1987).
10. P. Watkins *et al.*, *DNA* **6**, 205 (1987).
11. L. M. Davis *et al.*, *Genomics*, in press.
12. J. W. Moore *et al.*, *Hum. Genet.* **72**, 297 (1986).
13. L. M. Davis *et al.*, unpublished observations.
14. C. Turleau *et al.*, *Hum. Genet.* **67**, 455 (1984).
15. C. E. Rogler *et al.*, *Science* **230**, 319 (1985).
16. T. B. Shows *et al.*, *Somatic Cell Mol. Genet.* **10**, 315 (1984).
17. T. Maniatis, E. F. Fritsch, J. Sambrook, *Molecular Cloning: A Laboratory Manual* (Cold Spring Harbor Laboratory, Cold Spring Harbor, NY, 1982).
18. A. P. Feinberg and B. Vogelstein, *Anal. Biochem.* **132**, 6 (1983).
19. Our laboratory designations (11) for these clones are: *D11S89*, 57; *D11S90*, 530; *D11S91*, 679; *D11S92*, 684; *D11S93*, 706; *D11S94*, 1027; *D11S95*, 1104; *D11S200*, 63; and *D11S260*, 333.
20. F. Quan, R. G. Korneluk, M. B. Tropak, R. A. Gravel, *Nucleic Acid Res.* **14**, 5321 (1986).
21. R. G. Korneluk *et al.*, *J. Biol. Chem.* **259**, 13819 (1984).
22. We thank J. L. Yates for establishing the RIST cells in culture and for many discussions of this work and manuscript. We also thank M. Henry and L. Haley for the cell fusions, enzymatic analysis of the hybrids; and DNA isolations, and P. Watkins, R. Gravel, and C. Rogler for the *FSHB*, *CAT*, and *HVBS1* probes, respectively. Supported in part by American Cancer Society grant CD62 and NIH grants GM20454 and CA28853 to T.B.S.

12 April 1988; accepted 7 June 1988

Inactivation and Block of Calcium Channels by Photo-released Ca^{2+} in Dorsal Root Ganglion Neurons

MARTIN MORAD, NOEL W. DAVIES, JACK H. KAPLAN, H. DIETER LUX

Calcium channels are inactivated by voltage and intracellular calcium. To study the kinetics and the mechanism of calcium-induced inactivation of calcium channels, a "caged" calcium compound, dimethoxy-nitrophen was used to photo-release about 50 μM calcium ion within 0.2 millisecond in dorsal root ganglion neurons. When divalent cations were the charge carriers, intracellular photo-release of calcium inactivated the calcium channel with an invariant rate [time constant (τ) \approx 7 milliseconds]. When the monovalent cation sodium was the charge carrier, photorelease of calcium inside or outside of the cell blocked the channel rapidly ($\tau \approx$ 0.4 millisecond), but the block was greater from the external side. Thus the kinetics of calcium-induced calcium channel inactivation depends on the valency of the permeant cation. The data imply that calcium channels exist in either of two conformational states, the calcium- and sodium-permeant forms, or, alternatively, calcium-induced inactivation occurs at a site closely associated with the internal permeating site.

CALCIUM CHANNELS ARE HIGHLY Ca^{2+} selective. Currents carried by monovalent ions through the channel are blocked by low external Ca^{2+} concentrations ($2 \times 10^{-6}\text{M}$) (1, 2). Internal free Ca^{2+} also modulates the inactivation of the Ca^{2+} channel (3-6). However, little is known about the kinetics or the molecular mechanisms regulating these processes. We have examined the kinetics of interaction of Ca^{2+} with a neuronal Ca^{2+} channel by rapid "photo-release" of Ca^{2+} in the intra- or extracellular space from a novel caged Ca^{2+} compound, dimethoxy (DM)-nitrophen,

which on photolysis changes its Ca^{2+} -binding affinity.

Cultured chick (1- to 2-day-old) dorsal root ganglion (DRG) neurons were voltage clamped with the whole-cell patch clamp technique (7). Cells were dialyzed with internal solutions buffered either with EGTA to give an internal Ca^{2+} concentration

M. Morad and J. H. Kaplan, University of Pennsylvania, Department of Physiology, Philadelphia, PA 19104-6085.

N. W. Davies and H. D. Lux, Department of Neurophysiology, Max-Planck-Institute for Psychiatry, 8033 Planegg, Federal Republic of Germany.

Fig. 1. Photo-release of intracellular Ca^{2+} . **(A)** Ca^{2+} current through high-threshold Ca^{2+} channels in two different cells was suppressed following light-induced increase in $[\text{Ca}^{2+}]_i$. The external solution contained 120 mM NaCl, 5 mM CaCl_2 , 20 mM HEPES, and 3 μM (tetrodotoxin) TTX, at pH 7.3, and the pipette solution contained, in addition to high Cs^+ and HEPES concentrations, 2.25 mM DM-nitrophen and 2 mM CaCl_2 . The effect of a rapid increase in intracellular Ca^{2+} on the I_{Ca} is shown by the F traces. The C traces represent I_{Ca} before, and traces F + 1 are the I_{Ca} 3 s after, the photo-releasing light pulse. The time course of the effect caused by elevation of Ca^{2+} (traces F - C) was fitted by a single exponential with τ values of 6.83 and 7.69 ms, respectively. **(B)** A voltage-clamp ramp from +60 to -85 mV over 90 ms was applied immediately after a depolarizing command pulse and used to generate the I - V relation of the Ca^{2+} current before (trace C) and after (trace F) the photo-release of intracellular Ca^{2+} . The largest difference between curves C and F occurred at the peak of the I_{Ca} , indicating that the release of intracellular Ca^{2+} did not activate an outward or a nonspecific current. There was a larger flash artifact (A, right tracing) because a different voltage source for the light was used. In both cells the holding potential was -80 mV and the command potential was 0 mV.

